

The Gravitational Field of the Moon

Lunar satellite perturbations indicate striking correlations of gravity anomalies with ancient features.

William M. Kaula

This article concerns the distribution of mass in the moon, both radial and lateral; the measurement of the gravitational field; and the resulting questions of mass transfer, mass support, and density irregularities. Knowledge of the moon's gravity has increased greatly in recent years, mainly as a result of the accurate Doppler tracking of probes and lunar satellites by the Deep Space Network of the Jet Propulsion Laboratory (1). However, some older data are still of value, particularly heliometric measurements of the moon's librations (2) and photogrammetric measurements of the moon's shape (3).

I shall discuss, first the determination of parameters, in ascending order of complexity: mass, radius, moments of inertia, gravity anomalies, and topographic irregularities, and, second, the inferences drawn from these determinations with respect to the moon's structure and evolution.

Mass and Radius

One of the first results from space probes was a 30-fold improvement in the accuracy of the value for the ratio of the mass of the moon to that of the earth derived from the effect on the

tracking of the Mariner spacecraft of the motion of the earth about the earth-moon barycenter (1, 4). Further improvement in values for the product of the gravitational constant and the mass of the moon (GM) was obtained more directly from the attraction of the moon for approaching Ranger probes (1, 5). The current estimate for GM is 4902.78 ± 0.05 cubic kilometers per second per second.

The Ranger probes also contributed to the determination of an improved mean radius of the moon. The impacts of the probes were consistently later than those predicted by charts based on the photogrammetric control systems described below (6). These charts utilized a mean radius of 1738 kilometers determined from the occultations of stars by the moon's edge (7). The Ranger impacts indicated that the value for the mean radius (R) should be reduced to 1734.8 ± 0.3 kilometers. Further confirmation of this value is derived from the combination of the value of GM for the earth, the mean radar distance of the moon (8), and the mean motion of the moon in Kepler's equation. The mean density of the moon obtained from the values of GM and R given above and a value for G of $6.670 \pm 0.002 \times 10^{-8}$ cubic centimeter per gram per second per second is thus 3.361 ± 0.002 grams per cubic centimeter.

Cassini's Laws and Physical Librations

In 1693 Cassini observed that the moon obeyed, to a close approximation, three rules now known as Cassini's laws: (i) The rate of rotation of the moon equals its mean rate of revolution in its orbit about the earth; (ii) the lunar equator maintains a fixed inclination to the ecliptic, the plane of the earth's motion about the sun; and (iii) the moon's pole of rotation, the ecliptic pole, and the pole of the moon's orbit around the earth all fall in one great circle.

All three of Cassini's laws are apparently the consequence of a combination of torques exercised by the earth on the nonspherical shape of the moon and the imperfect elasticity of the moon, which results in the dissipation of the rotational energy of the moon and the transfer of rotational to orbital angular momentum until the extremum states constituted by Cassini's laws are attained.

The relevant equations are Euler's equations (rate of change of angular momentum equals torque) in a moon-fixed reference frame, with torques caused by the attraction of the earth for the irregularities in the moon's shape. These Euler equations to the first order, with dissipatory terms neglected, are:

$$\left. \begin{aligned} A\dot{\omega}_1 - (B - C)\omega_2\omega_3 &= 0 \\ B\dot{\omega}_2 - (C - A)\omega_3\omega_1 &= \frac{3GM^*}{r^3} \cdot (A - C)\lambda_3\lambda_1 \\ C\dot{\omega}_3 - \frac{3GM^*}{r^3}(B - A)\lambda_1\lambda_2 &= 0 \end{aligned} \right\} \quad (1)$$

Equation 1 is referred to right-handed rectangular coordinates with the 1-axis in the mean direction of the earth and the 3-axis in the mean rotation axis of the moon. With respect to these axes, A , B , C are the moments of inertia; ω_1 , ω_2 , ω_3 are the rates of rotation; λ_1 , λ_2 , λ_3 are the direction cosines of the earth; M^* is the mass of the earth; r is the distance of the earth; and overdots indicate derivatives with respect to time.

The author is professor of geophysics at the University of California, Los Angeles.

Of Cassini's three laws, the first law required the greatest energy dissipation. It occurred sometime in the past, when the moon's rotation was slowed to synchronization with its orbital revolution about the earth. In order to treat this problem, there must be added to the right side of the third line of Eq. 1 a tidal torque (T) much smaller than the torque on the fixed bulge ($B - A$) but of nonzero average because of its dependence on $\omega_3 - \dot{f}$, where \dot{f} is the angular rate of motion of the moon with respect to the earth.

Using a plausible form of the tidal torque dependence on the rate $\omega_3 - \dot{f}$, Goldreich (9) showed that the synchronous rotation sets a lower limit on $(B - A)/C$ relative to the orbital eccentricity at the time of trapping.

Once synchronous rotation was attained, in general there would have been a wobble of the direction of the rotation axis, which would interact with the torque dependent on $(C - A)$ in the second line of Eq. 1. By consideration of the adiabatic invariants related to energy and angular momentum, Colombo (10) and Peale (10) showed that, in the presence of dissipation, this wobble would be damped and the rotation axis of the moon driven to a location in accord with Cassini's second and third laws, with the final inclination a function of $(C - A)/B$. Peale also showed that there would be a negligibly small dependence on $(C - B)/A$.

Because the moon's orbit is eccentric, inclined, and perturbed by the sun, there is a variation in the torque exerted by the earth, which oscillates about ± 5 percent in distance and $\pm 7^\circ$ in direction with respect to the moon. This varying torque causes departures from Cassini's laws known as the physical librations. The mathematical expression of the varying torque is essentially a Fourier series expansion of the $\lambda_i \lambda_j / r^3$ parts of the right side of Eq. 1. Solutions of these equations either as linear perturbations (2) or by means of iterative techniques (11) exhibit annual and monthly oscillations in the physical libration with amplitudes of a few times 10 seconds of arc plus a 4.4-year oscillation which is resonant for a $(C - B)/(C - A)$ value of 0.662.

The principal observations related to the equatorial inclination and physical librations have been made on the heliometer, an astrometric telescope with a split objective lens which makes possible the measurement of angles between a selected point and the edge of the

moon's visible disk. Such observations with heliometers have been carried out in Germany and Russia over the past century. In the most comprehensive reduction of the data Koziel (2) obtained an equatorial inclination of $1^\circ 32' 1'' \pm 7.1''$ and a value for $(C - B)/(C - A)$ of 0.633 ± 0.011 , whence:

$$\left. \begin{aligned} (C - A)/B &= 0.000627 \pm 0.000001 \\ (B - A)/C &= 0.000230 \pm 0.000006 \end{aligned} \right\} \quad (2)$$

Some photogrammetric estimates of the physical librations have also been made. The principal method for the acquisition of improved data is ranging by laser to retrodirective reflectors on the moon, such as the one left by Apollo 11 (12). An accuracy of ± 15 centimeters is considered feasible. The values in Eq. 2, which were derived from heliometer observations, appear to be quite accurate enough to permit one to infer the mass distribution. The question we might hope to answer with more accurate data is whether the nonrigidity of the moon has a perceptible effect; that is, whether the laser ranging can make possible discrimination between different models of the lunar interior, such as those which postulate the presence or absence of a liquid core. Harrison (13) has calculated the effect of several such models in the form of the Love numbers k and h which give the ratios to the disturbing potential of the tidal potential (k) and the vertical displacement (h). The effects are disappointingly small: for a homogeneous moon with seismic velocities (v_{seismic}) comparable to the upper mantle of the earth, k is 0.020 and h is 0.034; for a fluid core radius 0.5 times the lunar radius, these values are modified to 0.038 and 0.068.

In order that we take into account the effect of the nonrigidity, the Euler equations (Eq. 1) must be generalized to allow for products of inertia and for the time variability of all components of inertia, and terms must be added which are k times the time-varying part of the earth's potential and the potential of the moon's rotation. These additional k -dependent terms can be viewed as modifications of the moments of inertia whose effect on the libration will be proportional to the effect of the total moments. Since this ratio is of the order of 10^{-6} , the effect is less than a centimeter (11). Another way of viewing the effect is that, for a forced oscillation of rate κ imposed on a system of free rate σ_0 , the modification of the amplitude will be $\kappa^2 / |\sigma_0^2 - \kappa^2|$. The moon's free period is about 20 minutes

($\sim 2\pi R / v_{\text{seismic}}$); thus for a monthly forced oscillation the modification factor is less than 10^{-6} .

Of more direct effect on the laser ranging will be the oscillation of the reflector due to tidal distortion of the moon. This effect will be of the order $h(GM^* R^2 / r^3) / g$, or about 40 centimeters, where g is the moon's gravitational acceleration. Hence some model discrimination may be possible, if care is taken in the calculation of the larger orbital and librational terms of the same periods.

Other techniques of obtaining more accurate information on lunar tides would be (i) long base-line radio interferometry (14) by use of a transmitter on the moon; and (ii) a gravity meter on the moon with an accuracy of about $\pm 10^{-6}$ centimeter per second per second (15).

Orbital Motion of the Moon

Cassini's law and the physical librations give values for $(C - A)/C$ and $(A - B)/C$. To obtain the physically more interesting quantity C/MR^2 , however, we need two dimensionless coefficients J_2 and J_{22} of the lunar gravitational field, definable as:

$$\left. \begin{aligned} J_2 &= [C - \frac{1}{2}(A + B)] / MR^2 \\ J_{22} &= (B - A) / 4MR^2 \end{aligned} \right\} \quad (3)$$

Until recently, the moon's own orbit was the only phenomenon sensitive to these terms, principally through the rates of precession $\dot{\Omega}$ of the node (the point of intersection of the orbit and the ecliptic), and $\dot{\omega}$ of the perigee (the point of closest approach to the earth). The "observed" rates are 1 revolution per 18.6 years, or $-6,967,943.6$ seconds of arc per century, for $\dot{\Omega}$, and 1 revolution per 8.9 years, or $+14,643,534.5$ seconds per century, for $\dot{\omega}$. All but about 800 seconds per century of this motion is caused by the sun; the planets contribute about 200 seconds per century, and the earth's oblateness J_2 contributes about 600 seconds per century, thus leaving a residual of less than 30 seconds per century that must be accounted for by the moon. Until the advent of artificial earth satellites, the earth's oblateness was too poorly known to permit one to distinguish the lunar effects. But a calculation at that time (1959) yielded an implausibly high value for C/MR^2 of 0.56, which suggests that the moon is closer to a hollow (0.67) than to a homogeneous (0.40) sphere. Investigators

therefore concluded that the solar contribution to $\dot{\Omega}$ postulated in the lunar theory of Brown was in error (16).

But the revision of Brown's theory by Eckert (17) left an even larger residual in $\dot{\Omega}$, -28 seconds per century, which resulted in the even more unreasonable value of 0.64 for C/MR^2 . This "hollow moon paradox" persisted for some years until van Flandern (18) pointed out that error lay not in Brown's theoretical $\dot{\Omega}$, but rather in his "observed" $\dot{\Omega}$, which he calculated as the difference of two quantities (19):

$$\dot{\Omega} = \frac{L_{1910} - L_{1750}}{1910 - 1750} - \frac{F_{1910} - F_{1840}}{1910 - 1840} \quad (4)$$

where L is the moon's longitude and F is the argument of latitude, the angle along the orbit from the node to the moon. In using these values over different time bases, Brown was making the implicit assumption that his "clock," the earth's rotation, had a uniform rate. But we now know that the earth's rotation varies, and on the basis of Brown's own values for the difference between the observed and calculated longitude of the moon, the mean rate for 1840 to 1910 is about 10 seconds per century less than the mean rate for 1750 to 1910 (20, p. 202). The application of this correction brings the value for C/MR^2 down to a comfortable 0.41. [But Brown (19) states that the latitude data are for 1847 to 1901, which would lower the value for C/MR^2 a good deal more. There is little doubt, however, that the matter will be resolved by the program of improved observation and analysis of the lunar motion being carried out by van Flandern and his associates.]

Lunar Satellite Orbit Analysis

Since 1966, 15 artificial satellites have been in orbit around the moon: five Lunas, five Lunar Orbiters, one Explorer, and four Apollos. Of these, only some of the Lunar Orbiters have combined all the desiderata for analyses to permit determinations of the variations in the lunar gravitational field: a small semimajor axis, accurate tracking, and long durations without disturbances by spacecraft outgassing. Some Lunar Orbiters have been maneuvered into more than one orbit, but their specifications can be listed in essentially seven groups, as summarized in Table 1. Of these seven, all but IVa may be used for the gravita-

Table 1. Lunar Orbiter satellite orbits of more than 7 days' duration.

Satellites	Lunar radii of the semimajor axis	Eccentricity	Inclination (deg)	Duration (days)
Iab, Iib	1.55-1.59	0.30-0.34	11.9-12.1	7- 65
IIcde	1.55-1.56	0.32-0.34	16.6-17.6	74-126
IIIbed	1.54-1.57	0.31-0.33	20.9-21.5	45- 95
IIIe	1.13	0.04	20.9	40
IVa	3.54	0.28	85.4	27
IVc	2.16	0.52	84.4	38
Vcd	1.46-1.63	0.28-0.32	84.6-85.1	63-112

tional measurements. However, they still fall far short of ideal in their distribution in inclination.

The initial plans (21) for the analysis of lunar satellite tracking were excessively influenced by experience with earth satellites. The determination of the earth's gravitational field from satellites has been based essentially upon perturbations arising from that part of the field which has not been "averaged out" in an orbital revolution. For most of the field, the averaging is done by the earth's rotation. In this situation, the convenient expression for the gravitational field is in the form of a sum of spherical harmonics for the gravitational potential V :

$$V(r, \varphi, \lambda) = \frac{GM^*}{r} \left[1 + \sum_{l=2}^{\infty} \sum_{m=0}^l (R^l/r) P_{lm}(\sin \varphi) \{C_{lm} \cos m\lambda + S_{lm} \sin m\lambda\} \right] \quad (5)$$

where r , φ , and λ are the radial, latitudinal, and longitudinal coordinates, respectively; $P_{lm}(\sin \varphi)$ is the Legendre-associated function: a polynomial with $(l-m)$ zeroes over the 180° range of φ ; and C_{lm} , S_{lm} are the independent coefficients which we attempt to determine by orbit analysis, using the gradients of V to obtain the accelerations needed in the equations of motion (22).

It was anticipated that the gravitational perturbations of lunar satellite orbits would be much larger than those of earth satellites (i) because the slower rotation has a significantly smaller averaging effect, and (ii) because the coefficients C_{lm} , S_{lm} will be larger in a smaller body, 36 times as large if equal stresses are assumed. To take advantage of all these effects, tracking would have to be done over at least a month at a time.

The various techniques applied (21) differed from each other in two main respects: the manner in which the equations of motion were integrated and the form in which the tracking data entered into the calculations. In

the analyses of Michael and his associates, the equations were integrated directly in rectangular coordinates, whereas in the analyses of Lorell and of Kaula, the orbit was calculated analytically with expressions for the perturbations in terms of the Kepler elements of the orbit (22). In the analyses of Michael and his associates and of Kaula, the tracking data were kept in the form of range rates, whereas in the analyses of Lorell, preliminary determinations of the orbits were made to obtain the day-by-day average values of the Kepler elements (a , e , I , ω , Ω); the variations of longer period in these average values were then used to determine the coefficients C_{lm} , S_{lm} .

The anticipation of sizable perturbations was more than fulfilled, to the extent that it was very difficult to obtain any stable solution. Contributory to this difficulty was the ill-conditioning that arose from the lack of variety of orbital inclination and the limitation of tracking to essentially one direction in a moon-fixed reference frame.

Given in Table 2 are the solutions made by Akim (23) based on tracking of Luna 10, of which he gives few details, solutions by Lorell and Sjogren (24), as well as the latest in a series of solutions by Michael and his associates (25). The solutions are given as normalized coefficients, C_{lm} , S_{lm} , corresponding to surface spherical harmonics $\bar{P}_{lm}(\sin \varphi) \{\cos m\lambda\}$ or $\bar{P}_{lm}(\sin \varphi) \{\sin m\lambda\}$, whose mean square value is unity. The solution of Michael *et al.* (25) was actually carried to the 13th degree. Given in Table 3, as a measure of variability of the field as a function of wavelength, is the degree variance σ_l^2 calculated from their coefficients:

$$\sigma_l^2 = \sum_{m=0}^l \{\bar{C}_{lm}^2 + \bar{S}_{lm}^2\} \quad (6)$$

The quantity $(C-A)/MR^2$ is determinable from the \bar{C}_{20} and \bar{C}_{22} values in Table 2 (Eq. 3 times normalization factors) as:

$$\frac{C-A}{MR^2} = \sqrt{5}(\bar{C}_{22}/\sqrt{3} - \bar{C}_{20}) \quad (7)$$

The $(C - A)/MR^2$ evaluated from the results of Michael *et al.* (25) together with the $(C - A)/B$ from Eq. 2 yield:

$$\frac{C}{MR^2} \approx \frac{B}{MR^2} = 0.402 \pm 0.002 \quad (8)$$

which is negligibly different from the value for a homogeneous body. The uncertainty is estimated mainly from the magnitude of the inadmissible harmonics, \bar{C}_{21} , \bar{S}_{21} .

To obtain the details of higher degree from the analysis of lunar satellite orbits, experience proved to be a poor guide; it was more than 1½ years after the launching of the first Lunar Orbiter that Muller and Sjogren (26) plotted systematically at intervals of 2° the range-rate residuals from the tracking of Lunar Orbiter V and then took the time derivatives of these residuals to obtain a map of accelerations over the visible face of the moon. This analysis resulted in the map which appeared on the cover of *Science* for 16 August 1968, which showed the marked correlation of downward accelerations with the five principal ringed maria, the "mascons."

The technique employed by Muller and Sjogren approximates the use of the lunar satellite as a direct accelerometer. Such a technique was proposed long ago for earth satellites and quickly discarded because tracking by one station never exceeds more than 20 minutes, the accelerations are too small, and too much of their effect would be absorbed by the constants of integration and errors in station position. But all these objections fade for lunar satellites: they can be tracked continuously for 90 minutes, a time sufficient for the determination of the constants of integration of a reference orbit for the range-rate residuals.

Figure 1 gives a map of the accelerations in the direction of the earth from the most recent analysis by Muller and Sjogren (27). The main defect of the technique is still a tendency to give spurious negative anomalies north and south of the principal mascon highs, as a consequence of absorption of some of the effect of the accelerations by the constants of integration. An excellent confirmation of the results of Muller and Sjogren was obtained by Wong *et al.* (28), who assumed the variations of the gravitational field to be caused by a set of mass points. However, their determination shares the defect of separate constants of integration for each north-south traverse of the satellite.

Table 2. Spherical harmonic coefficients (normalized) of the lunar gravitational field.

Coefficient	Akim (23) ($\times 10^{-6}$)	Lorell and Sjogren (24) ($\times 10^{-6}$)	Michael <i>et al.</i> (25) ($\times 10^{-6}$)
\bar{C}_{20}	-92.1	-90.6	-92.8
\bar{C}_{21}	-11.8	-6.6	-0.3
\bar{S}_{21}	-2.7	1.1	-3.5
\bar{C}_{22}	21.7	33.9	34.7
\bar{S}_{22}	-2.2	20.3	0.3
\bar{C}_{30}	-14.1	-8.6	-2.5
\bar{C}_{31}	52.6	33.7	22.6
\bar{S}_{31}	16.5	6.8	2.1
\bar{C}_{32}	34.6	-7.6	14.7
\bar{S}_{32}	-2.0	-5.9	5.9
\bar{C}_{33}		-19.3	11.9
\bar{S}_{33}	11.1	-35.8	-4.9
\bar{C}_{40}		3.1	6.4
\bar{C}_{41}		-13.1	-6.2
\bar{S}_{41}		5.9	7.2
\bar{C}_{42}		16.1	-4.3
\bar{S}_{42}		2.2	-6.7
\bar{C}_{43}		27.4	5.6
\bar{S}_{43}		-46.8	-9.4
\bar{C}_{44}		42.5	-5.2
\bar{S}_{44}		37.8	6.8
\bar{C}_{50}		-4.9	-2.3

Figures 2 and 3 show the map of radial accelerations calculated from the solution by Michael *et al.* in terms of spherical harmonic coefficients up through the 13th degree (25). The map of the front side shows some resemblance to the map of Muller and Sjogren (27), but the back side is much more extreme in its values. This difference suggests that the short periodic perturbations still have a major weight in the determination of coefficients in this solution, and that, as a result, the harmonics are a set of curves fitted to the data of the front side. The longest arc used by Michael *et al.* was 4 days.

In Figs. 4 and 5 are shown the accelerations calculated from the solution by Lorell and Sjogren in terms of spherical harmonics through the 4th

Table 3. Power spectrum of the lunar gravitational field.

Degree l	From coefficients of Michael <i>et al.</i> (25)		Predicted from earth's field
	σ_l^2 (Eq. 6) ($\times 10^{-12}$)	σ_l [$2l + 1$] ^½ ($\times 10^{-6}$)	σ_l [$2l + 1$] ^½ ($\times 10^{-6}$)
2	8620.	41.5	90.0
3	935.	11.6	40.0
4	386.	6.6	22.5
5	353.	5.7	14.4
6	912.	8.4	10.0
7	1767.	10.9	7.4
8	3429.	14.2	5.6
9	4691.	15.7	4.4
10	5554.	16.3	3.6
11	6895.	17.2	3.0
12	4599.	13.6	2.5
13	3014.	10.6	2.1

degree (24). The detail necessary to show the mascons is washed out, but the oscillations on the back side are not significantly larger, thus indicating that the longer periodic perturbations are being used. The problem of how to use the lunar satellites most effectively to determine the gravitational field on the back side of the moon must be regarded as still unsolved. Possible solutions are: (i) a greater variety of orbital inclinations; (ii) a satellite-to-satellite tracking system; (iii) satellite-borne laser altimetry; or (iv) satellite-borne measurements of gravity gradients.

Lunar Photogrammetry

The effective scientific utilization of the determinations of the gravitational field requires that the broad scale variations of topographic heights be determined to a comparable accuracy. The best determinations still depend on the measurements of plate coordinates of features on photographs taken by terrestrial telescopes (3). In these determinations, a few hundred control points are selected as being precisely identifiable, and their coordinates are measured on several plates: ideally, at least four plates are used in order that all extremes of the lunar optical libration, and the $\pm 7^\circ$ variation in the direction of the earth with respect to a moon-fixed reference system, be obtained. These plate coordinates then constitute the observations in an adjustment to determine the selenocentric coordinates of the control points plus the scale, orientation, and distortion parameters of the photographs. For the areas close to the edge of the visible disk, the measurements by Watts (7) are used, primarily for correction of occultation observations.

Of the various solutions (3), that by Meyer and Ruffin is probably superior in that existing photographs were selected, and new photographs taken, so as to obtain optimum variety of optical librations, uniform solar phase angle, and the best seeing conditions. Uncertainties in elevation probably vary from about ± 100 meters near the edge to about ± 750 meters near the center.

Attempts are now being made to utilize Lunar Orbiter IV photography for geodetic control on the moon (29). Appreciable improvement over the present situation will probably require a satellite-borne laser altimeter, which is planned for Apollo flights in 1971 and later.

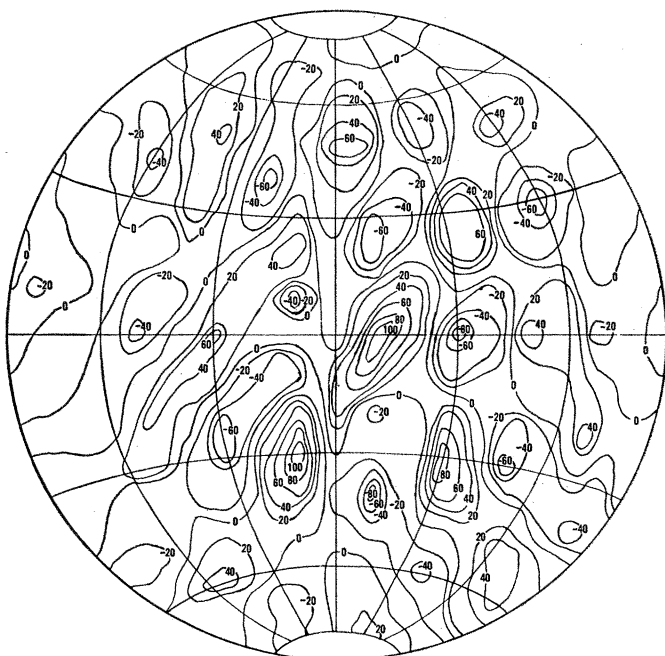
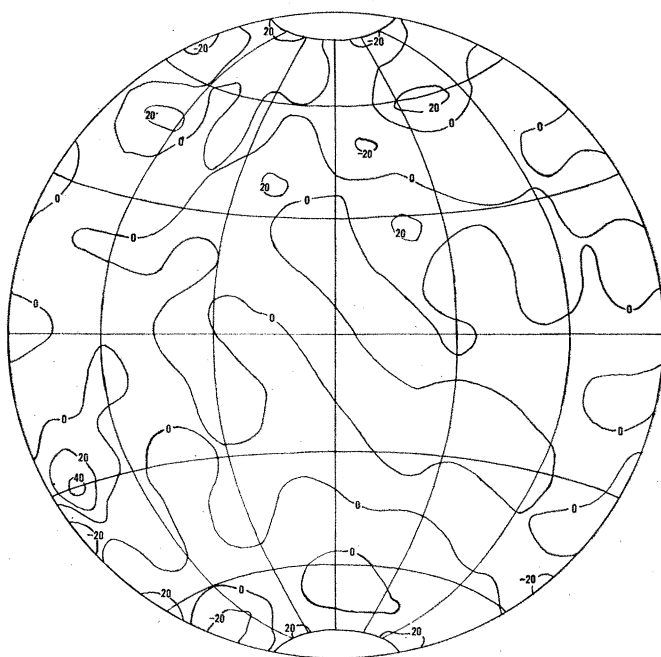


Fig. 1 (above left). Variations in gravitational acceleration on the front of the moon based upon Muller and Sjogren's analysis (27) of Doppler residuals. Unit equals 0.001 centimeter per second per second, or 1 milligal.

Fig. 2 (above right). Variations in gravitational acceleration on the front of the moon from the spherical harmonic coefficients of Michael *et al.* (25). Unit equals 0.001 centimeter per second per second, or 1 milligal.

Fig. 3 (left). Variations in gravitational acceleration on the back of the moon from the spherical harmonic coefficients of Michael *et al.* (25). Unit equals 0.001 centimeter per second per second, or 1 milligal.

Given in Fig. 6, for purposes of comparison with the gravitational field solutions, is the topographic solution of Baldwin (3), which utilizes the greatest number of control points, 696, and hence shows the most detail.

Interpretation

The mean density, 3.361 grams per cubic centimeter, obtained from the more accurate radius and mass values, merely confirms that the moon is significantly lighter than the earth, whose material would have a mean density of about 4.0 grams per cubic centimeter at comparable pressures. This differ-

ence is a fundamental datum of any theory of the moon's origin, being variously interpreted, relative to the earth, as attributable to the retention of silicates (which implies capture) (30), or to the loss of iron (which implies fission) (31).

The essential homogeneity of the moon, as indicated by a value for C/MR^2 so close to 0.40, suggests either that temperatures during the thermal history have remained too low to permit the separation of an iron core, or else that there was very little iron in the first place. The value of C/MR^2 and its uncertainty also place a crude upper limit of about 20 kilometers on the thickness of a basic (2.8 grams per

cubic centimeter) crust differentiated from an ultrabasic (3.4 grams per cubic centimeter) mantle.

The oblateness \bar{C}_{20} and equatorial ellipticity \bar{C}_{22} are both appreciably larger than would be compatible with hydrostatic equilibrium under the combined influences of rotation and the earth's attraction (32, p. 158). Because of the slow rotation and the absence of any geologic record of polar wander, the low values of \bar{C}_{21} , \bar{S}_{21} in Table 2 probably cannot be used to infer an upper limit on the viscosity, in a manner similar to that applied to the earth by Goldreich and Toomre (33). It is also dubious whether the large \bar{C}_{20} value bears any relation to the

variation with latitude of the moon's surface temperature (34).

The fact that the lower degrees of the spectrum in Table 3 have lower absolute magnitude than that predicted on the basis of the earth's gravity field under the equal-stress assumption indicates that the moon is closer to hydrostatic equilibrium than the earth, in the sense that the imbalance between disturbing effects (presumably dynamic) and restorative effects (presumably passive) is smaller. Because it is an imbalance, the gravitational field alone cannot be considered an indicator of primeval conditions; any such interpretation requires other data or assumptions. The lack of convergence in the

higher degrees of the lunar spectrum (Table 3) is undoubtedly the consequence of errors and distortion in the analysis of data. If it were real, it would suggest that the lunar gravitational field is much more the consequence of relatively local phenomena (such as asteroidal infalls) than of global phenomena (such as convection currents).

The mass concentrations on the moon manifested by the analyses of Muller and Sjogren (26, 27) are similar to the mass concentrations indicated by the earth's gravitational field in that the most marked departures from equilibrium are positive rather than negative. But lunar mascons are quite dif-

ferent from terrestrial mascons in that they are correlated (i) with topographic deficiencies rather than excesses, and (ii) with presumably ancient geology, the ringed maria, rather than with recent geology (35). The lunar mascons furnish corroboration for the lower degrees of the spectrum in that they indicate that the moon is appreciably closer to hydrostatic equilibrium than the earth: the excess mass indicated by the largest mascon in Table 4, Mare Imbrium, is exceeded by at least 20 terrestrial mascons, the excess being a factor of about 5 for the largest.

The existence of lunar mascons raises two questions that might also be raised with reference to terrestrial mascons:

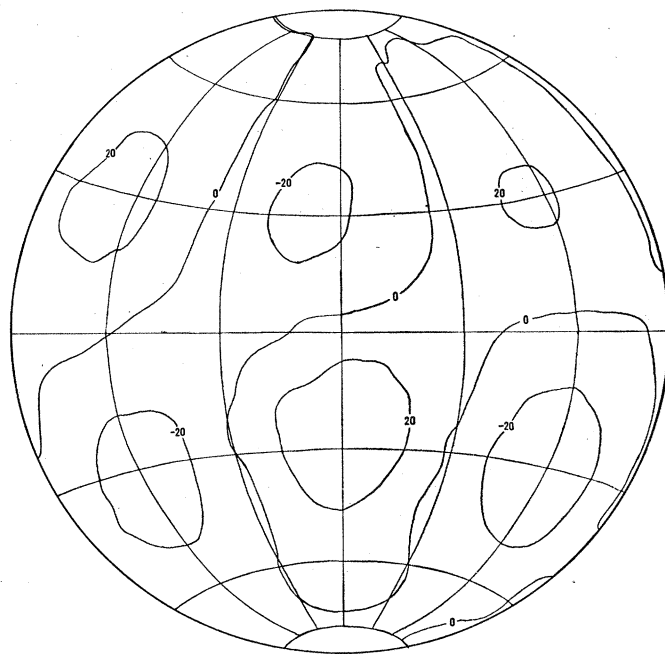
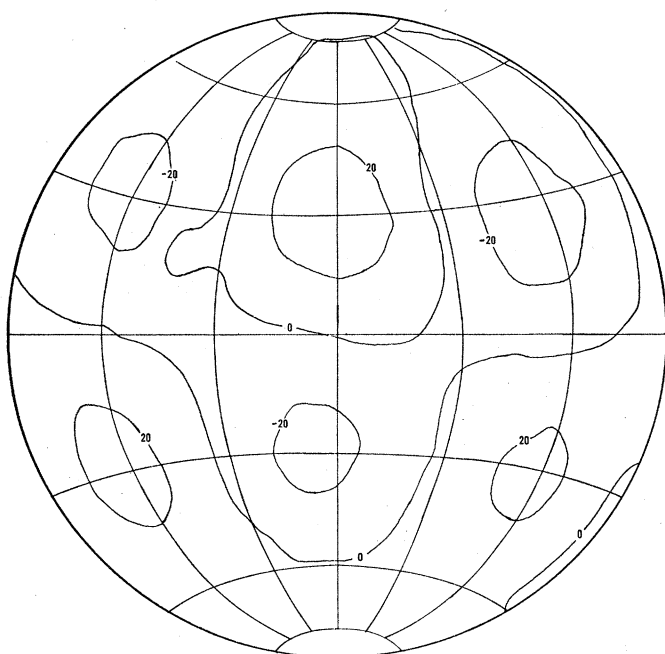


Fig. 4 (above left). Variations in gravitational acceleration on the front of the moon from the spherical harmonic coefficients of Lorell and Sjogren (24). Unit equals 0.001 centimeter per second per second, or 1 milligal.

Fig. 5 (above right). Variations in gravitational acceleration on the back of the moon from the spherical harmonic coefficients of Lorell and Sjogren (24). Unit equals 0.001 centimeter per second per second, or 1 milligal.

Fig. 6 (right). Variations in topographic elevation on the front of the moon from Baldwin (3). Unit equals 0.001 lunar radius, or 1.74 kilometers.

1) How was mass transferred to create the mass excess?

2) How has the mass excess been supported since it was transferred?

In addition, the negative correlation of gravimetry with topography raises a question peculiar to the moon:

3) Are there any mechanisms besides those associated with mass transfer which would make the ringed maria denser?

It is generally agreed that the ringed maria were created by infalling bodies early in the moon's history. However, in answer to the first question concerning mechanism of mass transfer, all possible responses are still supported:

1) The excess mass was brought in from outside the moon. Urey and MacDonald (36) propose that planetesimals of about the same mean density as the earth, 4.0 grams per cubic centimeter, were created in a terminal high-temperature stage of the formation. These bodies fell into the moon at very low velocity, creating the ringed maria and the mascons. The principal lunar evidences in favor of low-velocity impacts are (i) the absence of appreciable throwout associated with the ringed maria; and (ii) the distinct ellipticity of the maria Imbrium, Serengetatis, and Crisium. A difficulty associated with the hypothesis is that the circumstances of impacts with large bodies have not been worked out; simple scaled extrapolations from available data on nuclear explosions indicate that throwout mass is a factor of 20 times infall mass at the escape velocity of the moon, 2.4 kilometers per second (35). This throwout is undoubtedly an overestimate, but no one knows how much of an overestimate. It would be surprising if in the terminal stages of the moon's formation some sizable bodies did not fall in at velocities closer to the earth's orbital velocity—say, more than 10 kilometers per second. The most obvious site for such a high-velocity infall, Mare Orientale, is a small mascon.

2) The excess mass was transferred laterally on the surface of the moon. A necessary prelude to this process is that the moon differentiated (or acquired) a crust of lower density than the interior, so that when an infalling body created the preringed mare crater and threw out a lot of material, the mare remained a topographic depression after the crater had been isostatically compensated by a "root" of denser subcrustal material. The mass excess was then constituted by the sedi-

Table 4. Mass concentrations on the moon from Muller and Sjogren (27).

Feature	Latitude (°N)	Longitude (°E)	Peak anomaly (cm ² /sec)	Excess mass (× 10 ²¹ g)
Imbrium	38.	—18.	0.17	1.50
Serengetatis	28.	18.	.17	1.50
Crisium	16.	58.	.10	0.75
Nectaris	—16.	34.	.09	.70
Aestuum	10.	— 8.	.06	.45
Humorum	—25.	—40.	.05	.35
Humboldtianum	57.	82.	.04	.30
Orientale	—20.	—95.	.04	.30
Smythii	— 4.	85.	.04	.30
Nameless feature	— 7.	27.	.04	.30
Nameless feature	—17.	70.	.03	.22
Grimaldi	— 6.	—68.	.02	.15
Iridium	45.	—31.	—0.07	—0.50

ments which filled the basin. The difficulty in the hypothesis is finding an adequate erosion and sedimentation mechanism to account for the required 1 or 2 kilometers of excess material.

Gilvarry (37) proposed that the early moon had an atmosphere with an appreciable content of water. The usual objection is the lack of fluvial features on the moon. But perhaps a more fundamental objection is the amount of outgassing required. Gilvarry assumes that the moon was as efficient in outgassing as the earth, which implies a hot interior, perhaps too hot to permit the crust to cool off at depth in time to support the mass excesses necessarily laid down before the atmosphere escaped.

Gold (38) proposed that the mass was transferred by the downhill motion of fragments eroded by meteorite infall. However, in order that the mascons be created, the amount transported would have to be several orders of magnitude larger than values estimated from data now available (39).

3) The excess mass was transferred laterally inside the moon. This process also requires that the moon must have had a crust of lower density prior to the creation of the ringed maria. An essential to the process is an excess of internal pressure. Baldwin (40) and O'Keefe (40) suggested that this pressure is generated dynamically, as on earth, by convection, and that the greatest eruptions of lava have occurred on the ringed maria because they are places where the crust is weakest. But it is implausible that such an active lunar interior would produce excesses

coinciding so closely with ancient surface features, and the model is inconsistent with the evidence of low internal temperatures inferred by Ness (41) from the slight effect of the moon on transients in the solar wind.

Hence more passive sources of pressure have been sought. Wise and Yates (42) propose, as a source of pressure, the weight of the surrounding highlands, which forced lava over the mare floor after it had reached isostatic equilibrium by rise of a high-density root. This hypothesis requires that there be a negative ring around each mascon, of which there is some evidence; it also requires a thick crust (about 40 kilometers) and the simultaneous occurrence of local temperatures high enough to generate lava ($\approx 1100^\circ\text{C}$) and general temperatures low enough to allow strength to support the load ($\approx 700^\circ\text{C}$).

I have proposed (35) that the pressure was generated by thermal contraction, such as would have occurred if the outermost layer of the moon was hot enough to differentiate a crust while the interior was colder. The obvious objection is that the lithosphere would fail by a localized cracking. However, the process need only be about 0.1 percent efficient to provide sufficient pressure and would still continue when the moon had cooled enough to have a lithosphere several tens of kilometers thick. So the question becomes whether earthquakes of the shallow-focus type would remove the 10-bar (10^7 dynes per square centimeter) tensile stresses required in geologic time. The hypothesis neither requires nor precludes lava flows in the maria.

Finally, Peale and Lingenfelter (43) have suggested that there was instead a pressure deficiency at the surface associated with tides caused by the earth.

The mechanism for the subsequent support of the mascons is generally held (except by Baldwin and O'Keefe) to be the elastic strength of a lithosphere, which would be about 160 kilometers thick with temperature gradients of 5°C per kilometer (35). It has been estimated that maximum shear stresses under Mare Imbrium are about 60 bars (44).

The crustal differentiation required by most mascon hypotheses is corroborated by the alpha-scattering experiment of Turkevich *et al.* (45) and by chemical analyses of the Apollo 11 samples (46). Several densification mechanisms other than those neces-

sarily associated with the mass transfer may have operated, the most significant being dehydration, which would also result in increased thermal conductivity and hence lower thermal gradients in the maria (35).

Conclusions

In recent years studies of the gravitational field of the moon have generated several new clues on the moon's origin, history, and structure. The gross homogeneity of the moon seems well established; the moon is closer to equilibrium than the earth but far from completely inactive; the full explanation of the most intriguing features, the mascons, appears to require more detailed gravimetry measurements as well as other data; and more measurements are needed to provide the same accuracy for data related to the back side of the moon as for data related to the front side.

References and Notes

1. P. M. Muller and W. L. Sjogren, *Phys. Today* **22** (7), 46 (1969).
2. K. Koziel, in *Physics and Astronomy of the Moon*, Z. Kopal, Ed. (Academic Press, New York, 1962); *Icarus* **7**, 1 (1967).
3. R. B. Baldwin, *The Measure of the Moon* (Univ. of Chicago Press, Chicago, 1963); S. Breece, M. Hardy, M. Q. Marchant, *Army Map Serv. Tech. Rep.* 29 (1964); D. L. Meyer and B. W. Ruffin, *Icarus* **4**, 513 (1965); C. L. Goudas, *Advan. Astron. Astrophys.* **4**, 27 (1966); Z. Kopal, *Space Sci. Rev.* **4**, 737 (1965).
4. J. D. Anderson, G. W. Null, C. T. Thornton, in *Progr. Astronaut. Aeronaut.* **14**, 131 (1964); G. W. Null, H. J. Gordon, D. A. Tito, *Jet Propulsion Lab. Tech. Rep.* 32-1108 (1967).
5. C. G. Vegos and D. W. Trask, *Jet Propulsion Lab. Space Program Sum.* **3** (1967), p. 37.
6. W. L. Sjogren and D. W. Trask, *J. Spacecraft Rockets* **2**, 689 (1965).
7. C. B. Watts, *Astron. Pap. Amer. Ephemeris Nautical Almanac* **17**, 1 (1963).
8. B. S. Yapple, S. H. Knowles, A. Shapiro, K. J. Craig, D. Brouwer, *Bull. Astron.* **25**, 81 (1965).
9. P. Goldreich, *Astron. J.* **71**, 1 (1966).
10. G. Colombo, *ibid.*, p. 891; S. J. Peale, *ibid.* **74**, 483 (1969).
11. D. H. Eckhardt, *ibid.* **70**, 466 (1965); in *Measure of the Moon*, Z. Kopal and C. L. Goudas, Eds. (Reidel, Dordrecht, 1967).
12. C. O. Alley, P. L. Bender, R. M. Duke, J. E. Faller, P. A. Franken, M. M. Plotkin, D. T. Wilkinson, *J. Geophys. Res.* **70**, 2267 (1965); J. Faller, I. Winer, W. Carrion, T. S. Johnson, P. Spadin, L. Robinson, E. J. Wampler, D. Wieber, *Science* **166**, 99 (1969); C. O. Alley, P. L. Bender, D. G. Currie, R. H. Dicke, J. E. Faller, W. M. Kaula, G. J. F. MacDonald, J. D. Mulholland, H. H. Plotkin, S. K. Poultny, D. T. Wilkinson, in preparation.
13. J. C. Harrison, *J. Geophys. Res.* **68**, 4269 (1963).
14. B. F. Burke, *Phys. Today* **11** (7), 54 (1969); T. Gold, *Science* **157**, 302 (1967); I. I. Shapiro, *ibid.*, p. 806; M. H. Cohen, D. L. Jauncey, K. I. Kellermann, B. G. Clark, *ibid.* **162**, 88 (1968); M. H. Cohen, *Annu. Rev. Astron. Astrophys.* **7**, 619 (1969).
15. J. Weber, in *Physics of the Moon*, S. F. Singer, Ed. (American Astronomical Society Science and Technology Series 13, Tarzana, California, 1967), p. 181.
16. E. W. Brown, *Mem. Roy. Astron. Soc.* **53**, 39, 163 (1897); *ibid.* **54**, 1 (1899-1901); *ibid.* **57**, 51 (1908); *ibid.* **59**, 1 (1908); A. H. Cook, *Geophys. J. Roy. Astron. Soc.* **2**, 222 (1959); H. Jeffreys, *Mon. Notic. Roy. Astron. Soc.* **122**, 421 (1961).
17. W. J. Eckert, *Astron. J.* **70**, 787 (1965).
18. T. C. van Flandern, *Jet Propulsion Lab. Tech. Rep.* 32-1247 (1968), p. 13.
19. E. W. Brown, *Mon. Notic. Roy. Astron. Soc.* **75**, 510 (1915).
20. W. H. Munk and G. J. F. MacDonald, *The Rotation of the Earth* (Cambridge Univ. Press, New York, 1960).
21. W. M. Kaula, in *Measure of the Moon*, Z. Kopal and C. L. Goudas, Eds. (Reidel, Dordrecht, 1967); J. Lorell, in *ibid.*, p. 356; W. H. Michael, Jr., and R. H. Tolson, in *The Use of Artificial Satellites for Geodesy*, G. Veis, Ed. (National Technical University, Athens, 1967), vol. 11, p. 609.
22. W. M. Kaula, *Theory of Satellite Geodesy* (Blaisdell, Waltham, Mass., 1966).
23. E. L. Akim, *Dokl. Akad. Nauk SSSR* **170**, 799 (1966).
24. J. Lorell and W. L. Sjogren, *Science* **159**, 625 (1968).
25. W. H. Michael, Jr., W. T. Blackshear, J. P. Gapcynski, in *COSPAR Space Research 10* (North-Holland, Amsterdam, in press).
26. P. M. Muller and W. L. Sjogren, *Science* **161**, 680 (1968).
27. ———, in *COSPAR Space Research 10* (North-Holland, Amsterdam, in press).
28. L. Wong, W. Downs, G. Buechler, R. Prislun, *Aerospace Corp. Rep. ATR-69(7140)-1* (1969).
29. U.S. Air Force Aeronautical Chart and Information Center, *Lunar Photomap Development Study* (U.S. Air Force Aeronautical Chart and Information Center, St. Louis, 1969).
30. H. C. Urey, *The Planets* (Yale Univ. Press, New Haven, 1952); *Phys. Chem. Earth* **2**, 46 (1957); in *Space Science*, D. P. LeGalley, Ed. (Wiley, New York, 1963).
31. A. E. Ringwood, *Geochim. Cosmochim. Acta* **30**, 41 (1966).
32. H. Jeffreys, *The Earth* (Cambridge Univ. Press, New York, ed. 3, 1952).
33. P. Goldreich and A. Toomre, *J. Geophys. Res.* **74**, 2555 (1969).
34. V. S. Safranov, *Icarus* **7**, 275 (1967).
35. W. M. Kaula, *J. Geophys. Res.* **74**, 4807 (1969); *Phys. Earth Planet. Interiors*, **2**, 123 (1969).
36. H. C. Urey, *Science* **162**, 1408 (1968); ——— and G. J. F. MacDonald, in *Physics and Astronomy of the Moon*, Z. Kopal, Ed. (Academic Press, New York, ed. 2, 1969).
37. J. J. Gilvarry, *Nature* **188**, 804 (1960); *ibid.* **221**, 553, 732 (1969).
38. T. Gold, personal communication.
39. H. P. Ross, *J. Geophys. Res.* **73**, 1343 (1968).
40. R. B. Baldwin, *Science* **162**, 1407 (1968); J. A. O'Keefe, *ibid.*, p. 1405.
41. N. F. Ness, *Trans. Amer. Geophys. Union* **50**, 216 (1969).
42. D. U. Wise and M. T. Yates, *J. Geophys. Res.*, in press.
43. S. J. Peale and R. E. Lingelfelter, personal communication.
44. J. E. Conel and G. B. Holstrom, *Science* **162**, 1403 (1968).
45. A. L. Turkevich, E. J. Franzgrote, J. H. Patterson, *ibid.*, p. 117.
46. Lunar Sample Preliminary Examination Team, *Science* **165**, 1211 (1969).
47. Supported by NASA grant NGL 05-007-002. Publication No. 763, Institute of Geophysics and Planetary Physics, University of California, Los Angeles.

Chemoreceptors in Bacteria

Studies of chemotaxis reveal systems that detect attractants independently of their metabolism.

Julius Adler

Motile bacteria are attracted to a variety of chemicals—a phenomenon called chemotaxis [for a review, see (1)]. Although chemotaxis by bacteria has been recognized since the end of the 19th century, thanks to the pioneering work of Engelmann, Pfeffer, and other biologists, the mechanisms involved are still almost entirely unknown. How do

bacteria detect the attractants? How is this sensed information translated into action; that is, how are the flagella directed? This article deals primarily with the first question.

To learn about the detection mechanism that bacteria use in chemotaxis, it is important first to know *what* is being detected. One possibility is that

the attractants themselves are detected. In that case, extensive metabolism of the attractants would not be necessary for chemotaxis. There is another possibility: the attractants themselves are not detected but, instead, some metabolite of the attractants is detected (for example, the pyruvate inside the cell); or the energy produced from the attractants, perhaps in the form of adenosine triphosphate, is detected. In these cases, metabolism of the attractants would be necessary for chemotaxis. The idea that bacteria sense the energy produced from the attractants has, in fact, gained wide acceptance for explaining chemotaxis (and also phototaxis) (2).

To try to determine which of these possibilities is correct, experiments were carried out with *Escherichia coli* bacteria, which had previously been